Propagation Characteristics for Wideband Outdoor Mobile Communications at 5.3 GHz

Xiongwen Zhao, Jarmo Kivinen, Pertti Vainikainen, *Member, IEEE*, and Kari Skog

***Abstract*—In this paper, empirical channel models and parameters are derived from the wideband measured data at 5.3 GHz in outdoor mobile communications. The path loss exponents and intercepts are obtained by using the least square method. The mean excess delay and mean root-mean-square (rms) delay spread are within 29–102 ns and 22–88 ns, respectively. The correlation distances and bandwidths are within 1–11λ and 1.2–11.5 MHz, respectively, when the envelope correlation coefficients equal 0.7 in line-of-sight cases. These correlation values depend strongly on the base station antenna heights. The window length for averaging out the fast fading components is about 1–2 m for microcells and picocells. The multipath number distributions follow both Poisson's and recently introduced Gao's distributions, but Gao's distribution is better at high probability region. Large excess delays up to 1.2 μs and rms delay spread about 0.42 μs are found in the urban rotation measurements, where the receiver is close to a large open square.**

***Index Terms*—Correlation, delay spread, multipath propagation, path loss, path number distribution, radio channel.**

I. Introduction

THE WIRELESS local area networks (WLANs) directed to communications between computers, of which High-Performance LAN (HIPERLAN) [1] and IEEE 802.11 [2] are examples, and mobile broadband system (MBS) [3], intended as a cellular system providing full mobility to broadband integrated services digital network (ISDN) users. The HIPERLAN committee has identified the 5.15–5.30 GHz and 17.1–17.2 GHz bands for transmission and 5 GHz band has been ratified for HIPERLAN use by CEPT (the Conference of European Postal and Telecommunications Administrations) [1], [4]. Therefore, the channel experiments and modeling are quite important at 5-GHz frequency bands. However, there are not enough experiments and modeling work reported at this frequency band in open literature at present, especially in outdoor environments [5]–[7]. In this paper, based on the experimental data, path loss models are derived by using the least square method, which can be directly used in coverage analysis. Excess delay and rms delay spread are the basic modeling parameters, e.g., the rms delay spread is directly connected to the capacity of a specific communication system and gives a rough implication on the complexity of a receiver. The adaptive antenna array and diversity techniques are sensitive to correlation properties of signals. Therefore, spatial and frequency correlation studies are needed. The mobile radio channel is a typical multipath propagation channel, so the path number distribution is one of the important channel characteristics to study. It is useful in the computer simulation, interference analysis and studying the other multipath propagation properties for a specific communication system.

The radio channel is characterized by its time-variant complex impulse responses (IRs) $h(\tau, t)$, where τ and t denote the measurement delay and time, respectively, and

$$h(\tau, t) = \sum_{i=1}^{N} h_i(t)\delta[\tau - \tau_i(t)] \tag{1}$$

where h_i is the complex amplitude of a signal arriving via discrete propagation path i with delay τ_i. The radio channel is time variant, so in order to study the small scale effects of the radio channel, such as spatial and frequency correlation properties, a wide sense stationary uncorrelated scattering (WSSUS) channel should be assumed. Due to multipath propagation characteristics for mobile radio channel the received signal contains fast fading components, and one important question is how to choose a suitable window length to average the fast fading components and still preserve the slow fading properties. The window lengths were discussed in [8] and [9] for macro- and microcellular mobile communications, respectively. However, for micro- and picocells, the window length is not quite clear at present. Concerning estimation of direction of arrival of the waves, one of the simplest methods is to use a directive rotated antenna with narrow beam-width, and the rotation measurement is also a useful method for studying the other spatial propagation characteristics of a specific environment.

This paper is structured as follows. In Section II, the measurement campaign is introduced. The empirical path loss models are derived in Section III with different transmitter heights. The statistical values of excess delay and rms delay spread are derived in Section IV. In Section V, the suitable window length is introduced for averaging out fast fading components in both the wide and narrowband signals. The spatial and frequency correlations, and path number distributions are studied in Sections VI and VII, respectively. In Section VIII, the results for the rotation measurement are illustrated. Finally, the conclusions are drawn in Section IX.

II. Measurement Campaign

The outdoor mobile measurements at 5.3 GHz were performed in Helsinki, Finland [7]. The measurements in urban, suburban, and rural environments were performed with different transmitting antenna [base station (BS)] heights. For urban measurements, three transmitter sites were chosen. Site A

Manuscript received March 15, 2001; revised August 29, 2001. This work was supported in part by the Academy of Finland, Helsinki, Finland. This paper was presented in part at the 4th European Personal Mobile Communications Conference, Vienna, Austria, February 20–22, 2001

X. Zhao, J. Kivinen and P. Vainikainen are with the Radio Laboratory, Institute of Digital Communications, Helsinki University of Technology, Espoo FIN-02150 HUT, Finland. (e-mail: xzh@radio.hut.fi).

K. Skog is with the Nokia Research Center, Radio Communications, Helsinki 00045, Finland.

Publisher Item Identifier S 0733-8716(02)03292-4.

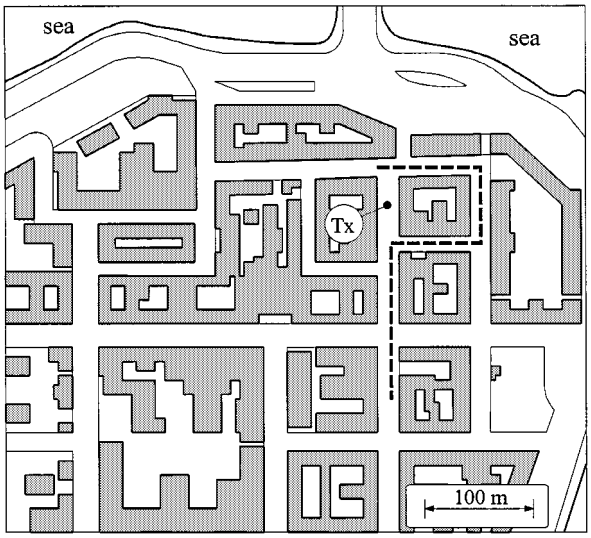

Fig. 1. Measurement routes for Site B with Tx height of 4 m.

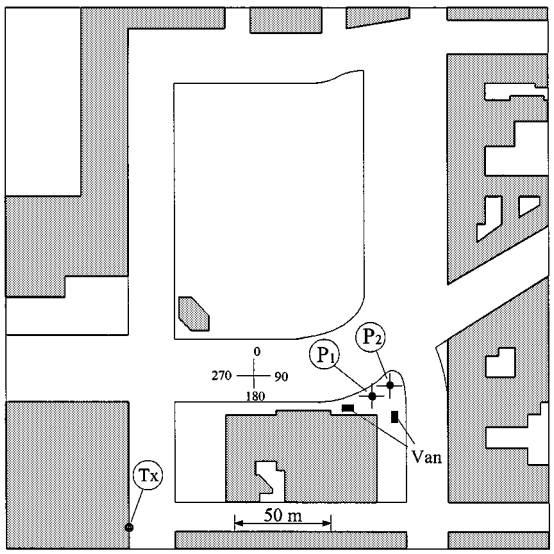

Fig. 2. Rotation measurements in an urban environment.

is an example of a dense urban environment, the transmitting antenna was about 45 m above ground level representing a case with the BS antenna over rooftops. Site B is a dense urban residential environment. Here the transmitting antenna was placed at a mast with a height of 4 m, which is a typical case with the BS antenna lower than rooftops. The measurement routes for this site are shown in Fig. 1. The receiving antenna mobile station was at the height of 2.5 m on top of a car for both of the sites mentioned above. Site C is located in the city center of Helsinki. The goal was to place the transmitter at some elevation relative to ground, but still keep it below rooftops. The transmitting antenna was placed at the height of 12 m and the receiving antenna was on top of a trolly with the height of 2 m above ground level. In Site C, we also did the rotation measurements by using a directive horn antenna. The 3 dB beamwidth of the horn antenna was 30° in H-plane and 37° in the E-plane and the peak sidelobe level was 26 dB. The specific environment for rotation measurements is shown in Fig. 2. Site D represents semiurban/semirural residential area. The three-story buildings are the tallest ones around, and the transmitting antenna was placed over rooftops at the height of 12 m from ground level. Site E was selected to represent the rural case. The transmitting antenna was placed on top of a 5 m mast at the hilltop so that the antenna was about 55 m above the surroundings. Site F represents a typical semiurban/urban case. The transmitter was placed on top of a 5 m mast. The receiving antenna was always on top of a car at the height of 2.5 m. The routes were measured by using the wideband channel sounder developed at the Institute of Digital Communications in Helsinki University of Technology [10]. In the measurements, more than 200 000 useful IRs were collected. The system configuration for mobile measurements is described in Table I.

TABLE I
SYSTEM CONFIGURATION FOR MOBILE MEASUREMENTS

Receiver	Direct sampling / 5.3 GHz
Transmitter power	30 dBm
Chip frequency	30 MHz
Delay range	4.233 μs
Doppler range	124 Hz (U), 62 Hz (S, R)
Measurement rate	248 sets/s (U), 124 sets/s (S, R)
Sampling frequency	120 Ms/s
IRs / wavelength	5 (U), 4.2 (S, R)
Receiver velocity	2,8 m/s (U), 1.67 m/s (S, R);
Antennas and polarization	Omni-directional antenna with 1 dBi gain; Vertical polarization

TABLE II
PATH LOSS MODELS FOR URBAN ENVIROMENTS

Urban	Tx height: 4 m			Tx height: 12m			Tx height: 45m		
Models	n	b (dB)	std(dB)	n	b (dB)	std(dB)	n	b (dB)	std(dB)
LOS	1.4	58.6	3.7	2.5	35.8	2.9	3.5	16.7	4.6
NLOS	2.8	50.6	4.4	4.5	20.0	1.7	5.8	-16.9	2.8

TABLE III
PATH LOSS MODELS FOR SUBURBAN AND RURAL ENVIRONMENTS

Models	Rural Tx height: 55 m			Suburban LOS: (Tx height: 5 m), NLOS: (Tx height 12 m)		
	n	b (dB)	std (dB)	n	b (dB)	std (dB)
LOS	3.3	21.8	3.7	2.5	38.0	4.9
NLOS	5.9	-27.8	1.9	3.4	25.6	2.8

III. PATH LOSS MODELS

The least square method is used in the derivation of empirical path loss models at different transmitter heights in outdoor environments. The following model [11]–[13] was utilized for wideband path loss with isotropic antennas

$$PL(\text{dB}) = b + 10n\log_{10} d \tag{2}$$

where $d_0 = 1$ m, n is attenuation exponent, b is the intercept point in the semilog coordinate, and $d(m)$ is the distance from receiver to transmitter. The dynamic range is cut at -20 dB in the delay domain relative to the strongest path in Sections III–VII of this paper. The empirical path loss models are given in Tables II and III for urban, suburban and rural environments, respectively. The measurement distances are about 30–300 m in this measurement campaign. In line-of-sight

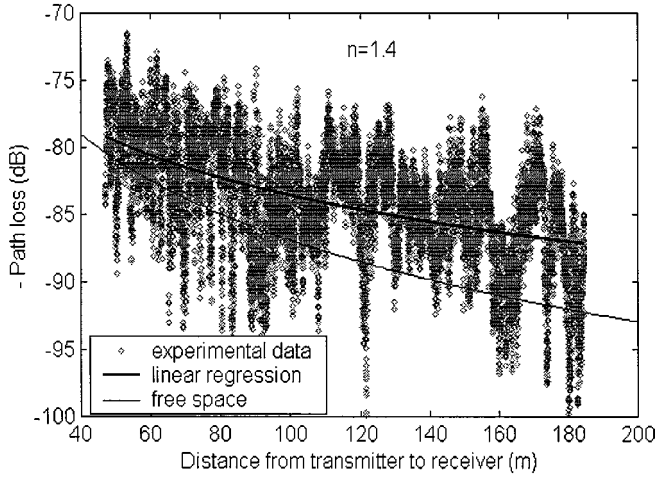

Fig. 3. Path loss for urban LOS with Tx height of 4 m.

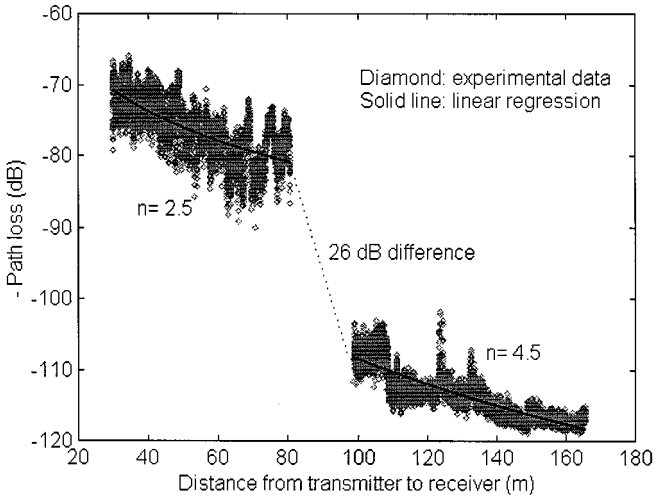

Fig. 4. Mobile terminal turning around a corner with Tx height of 12 m in an urban environment.

(LOS) cases, the attenuation exponent n is in the range of 1.4–3.5 and in nonline-of-sight (NLOS) cases n is 2.8–5.9. Two examples are shown here. Fig. 3 shows urban LOS path loss when transmitter was at a mast 4 m above ground. Due to guided wave effect the average signal level is higher than in free space. Fig. 4 shows a mobile terminal turning around a corner. More than 25 dB path loss difference can be found from LOS to NLOS situations.

IV. Measured Values for Excess Delay and rms Delay Spread

By using the basic theory introduced in [14], the empirical values for mean excess delay and rms delay spread shown in Table IV can be derived from the measured data. Here both transmitter (Tx) and receiver (Rx) had omni-directional antennas. Two examples are given here. Fig. 5 shows the rms delay spread as a function of the distance between Tx and Rx for suburban LOS case with Tx height of 5 m. Fig. 6 is for urban NLOS case with Tx height of 4 m. The time resolution of the measurement setup limits the minimum measurable rms delay spread to about 10.5 ns. As shown in Table IV, in the

TABLE IV
Measured Values for Mean Excess Delay and Rms Delay Spread

( ) Tx height in meters			Urban		Suburban		Rural	
Mean excess delay (ns)	LOS		38 42 102	(4) (12) (45)	36	(5)	29	(55)
	NLOS		70	(4)	68	(12)		
Rms delay spread (ns)	Mean	LOS	44 41 88	(4) (12) (45)	25	(5)	22	(55)
		NLOS	44	(4)	66	(12)		
	Median	LOS	25 31 86	(4) (12) (45)	13	(5)	15	(55)
		NLOS	37	(4)	63	(12)		
	CDF <90%	LOS	93 64 120	(4) (12) (45)	57	(5)	44	(55)
		NLOS	63	(4)	105	(12)		

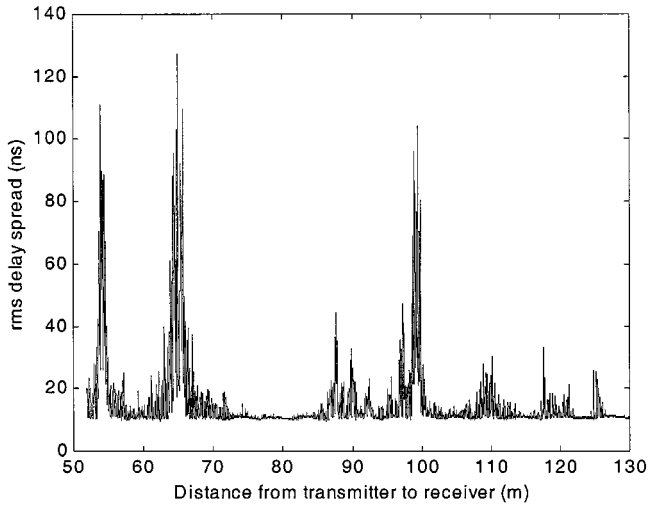

Fig. 5. Rms delay spread for suburban LOS with Tx height of 5 m.

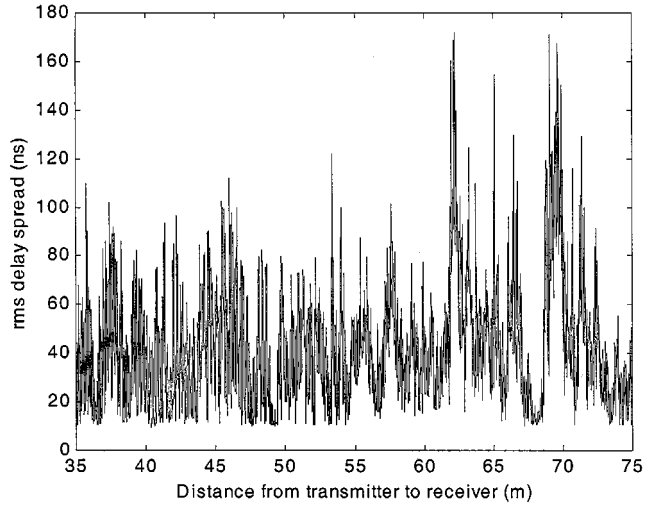

Fig. 6. Rms delay spread for urban NLOS with Tx height of 4 m.

outdoor environments the mean excess delay and mean rms delay spread are within 29–102 ns and 22–88 ns, respectively, and the values depend on the transmitter heights and LOS or NLOS situations. Generally speaking, the mean excess delay and rms delay spread are higher with the increasing Tx heights. However, in rural LOS measurement, when the transmitter was placed on a hill, the mean excess delay and rms delay spread

are small, which can be explained by the fact that there are no high buildings to reflect the radio waves, and only some scattered waves from nearby cars and trees exist. The rotation measurements in Section VIII will show that large excess delays up to 1.2 μs and rms delay spread about 0.42 μs can be found in urban NLOS case with Tx height of 12 m and the Rx is close to a large open square with surrounding buildings.

V. Window Length for Averaging Fast Fading Components at 5 GHz

Multipath propagation causes fast fading in mobile communications. Thus, it is quite important in experimental data processing how to average out the fast fading components and still preserve the slow fading characteristics. In [8], it was suggested that a suitable window length for data taken from macrocells is 40λ. However, examination of data taken from microcells showed that the local mean could suffer quite large variations over short distances and in [9], 5λ (about 1.7 m) was considered more appropriate window length for microcells from the experimental data at 900 MHz. In our experiments, we used the least square method with the wide and narrowband received power to give the linear regression curves. Let's take the regression curves as the reference values, and then change the window length to 5, 10, 20, and 40λ for averaging the fading signals. Fig. 7(a) shows the wideband received power for urban LOS with the transmitter height of 12 m. If we now take the linear regression values as the average received power, the standard deviations (std) are 2.47, 2.25, 1.93, and 1.62 dB corresponding to the window lengths of 5, 10, 20, and 40λ, respectively. It is seen that the fast fading components are averaged out if the window length is in the range from 20λ to 40λ, namely, 1–2 m. The same conclusion can also be obtained for averaging narrowband fast fading components and the corresponding result can be found in Fig. 7(b). So, based on [9] and the experience of processing much measured data at 5 GHz, it seems that the practical window length for averaging out fast fading components is 1–2 m in micro- and pico-cells at 900 MHz–5 GHz frequency bands.

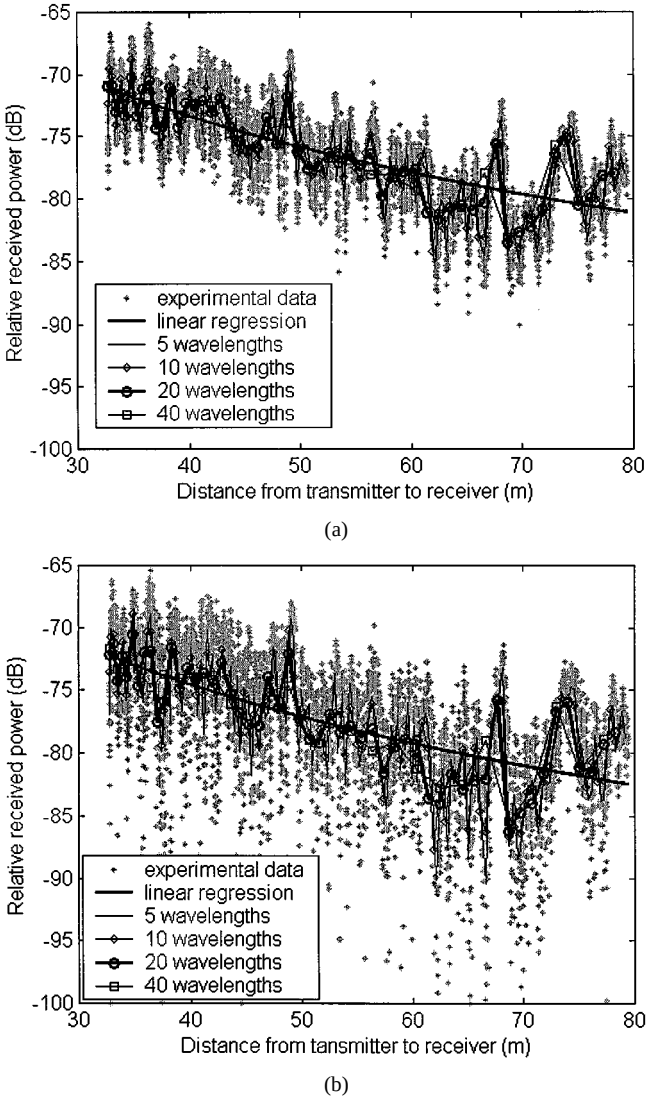

Fig. 7. Window length for averaging out fast fading components at 5.3 GHz. (a) Wideband. (b) Narrowband.

VI. Spatial and Frequency Correlations

Spatial and frequency correlation study is useful for the design of antenna diversity to reduce the multipath fading. Because the correlation behavior is a small scale effect, a wide sense stationary uncorrelated scattering (WSSUS) situation should be assumed. To meet this condition, here 200 IRs (about 40λ) used as the window length to give the average correlation function. The formulas for calculating spatial and frequency correlation functions can be found in [15], [16]. In this paper, envelope correlation is considered for narrowband signals. However, recent research [17] has shown that spatial correlation characteristics do not largely depend on frequency bandwidth up to approximately 20% of the carrier frequency ($B/f_c = 0.2$, where B is the bandwidth of a transmitted signal and f_c is the carrier frequency). Therefore, the narrowband model is sufficient for computing the spatial correlation characteristics within $B \leq 0.2 f_c$.

Figs. 8(a) and (b) and 9(a) and (b) show the spatial and frequency envelope correlation functions for LOS outdoor environments at different transmitter heights. It is seen that the correlation distances are strongly dependent on the transmitter heights. The correlation distances with the envelope correlation coefficient of 0.7 are between 1 to 11λ (about 0.06–0.62 m). The respective correlation bandwidths are between 1.2 to 11.5 MHz. In LOS cases, due to the direct wave superimposed by only weak scattered waves, the coherence is high and the correlation length is large.

VII. Path Number Distribution

The multipath number distribution was regarded as Poisson's and modified Poisson's distributions in [18] and modified Poisson's distribution has been shown to have good agreement with the experimental results in some cases. However, the modified Poisson's distribution does not have an explicit expression, but just a process. Therefore, it is not convenient for practical use. In [19] and [20], another simple and useful path number distribution was derived by considering the path number variation of radio waves in land mobile communications is a

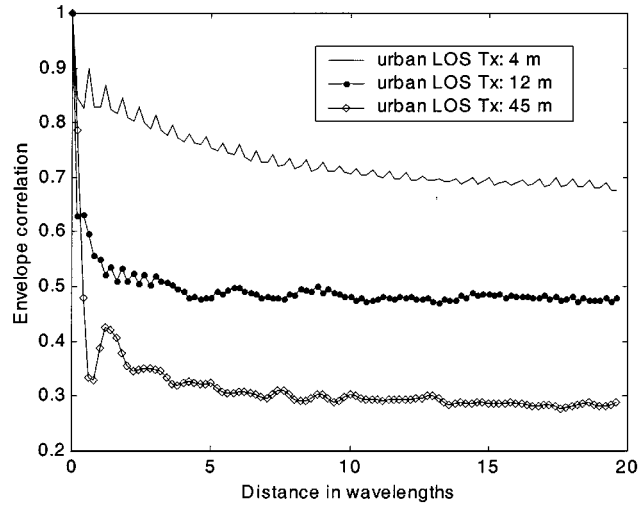

(a)

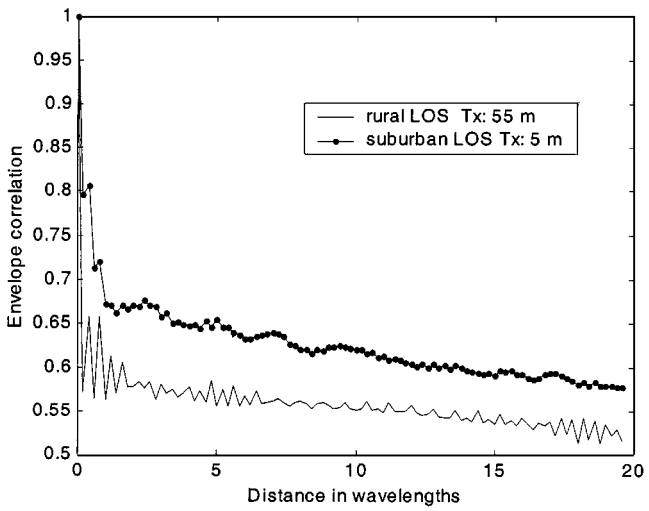

(b)

Fig. 8. Spatial correlations in LOS outdoor environments. (a) Urban cases with three transmitter heights. (b) Rural and suburban cases with two transmitter heights.

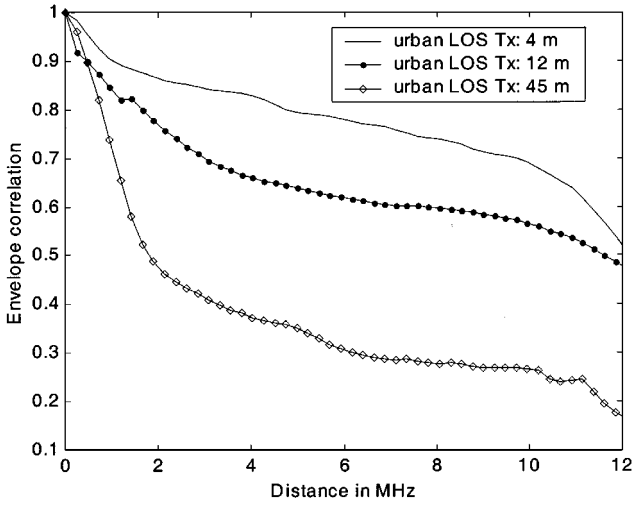

(a)

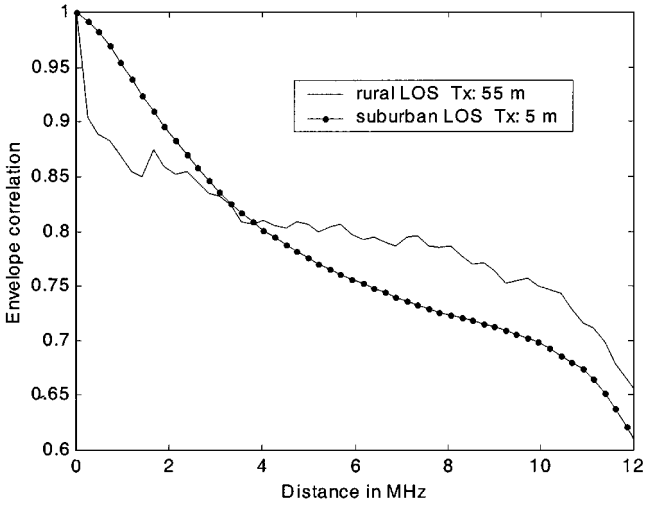

(b)

Fig. 9. Frequency correlations in LOS outdoor environments. (a) Urban cases with three transmitter heights. (b) Rural and suburban cases with two transmitter heights.

Markov process at finite state space, and it was shown to have good agreement with the experimental results. The path number distributions given by Poisson and Gao can be expressed as

$$P(N) = \frac{\eta^{N_T - N}}{(N_T - N)!} e^{-\eta} \tag{3}$$

$$P(N) = C_{N_T}^{N} \frac{\eta^{N_T - N}}{(1+\eta)^{N_T}} \tag{4}$$

where N is variable and C means combination. N_T is the maximum number of paths that the mobile can receive. The parameters η and N_T can be fitted by the experimental data. For Poisson's probability density function (PDF), the mean path number is $\langle N \rangle = \eta$. For Gao's PDF, the mean value is $\langle N \rangle = N_T/(1+\eta)$. The empirical path number distributions for the outdoor measurements are fitted by using (3) and (4), respectively. The path numbers are obtained from measured data by counting the peaks of the power delay profiles. The best fit is obtained by minimizing the following standard deviation

$$\text{std} = \sqrt{\frac{1}{N_T} \sum_{i=1}^{N_T} (p^i - p_e^i)^2} \tag{5}$$

where p_e^i is the experimental probability corresponding to path number i and p^i is the fitted probability by using (3) and (4). The fitted parameters are available in Table V. Fig. 10(a)–(c)

TABLE V
PATH NUMBER DISTRIBUTIONS FOR OUTDOOR ENVIRONMENTS

		Urban				Suburban		Rural
		Tx 4 m		Tx 12 m	Tx 45 m	Tx 12 m		Tx 55 m
		LOS	NLOS	LOS	LOS	LOS	NLOS	LOS
η	Poisson	2.8	4.2	3.3	6.0	1.2	4.5	1.8
	Gao	4.7	4.5	3.5	2.7	9.0	3.3	4.0
N_T		16	21	14	22	13	20	9
$\langle N \rangle$	Poisson	2.8	4.2	3.3	6.0	1.2	4.5	1.8
	Gao	2.8	3.8	3.2	6.0	1.3	4.7	1.8
	Experiment	3.4	4.2	3.5	6.2	2.4	5.0	1.7

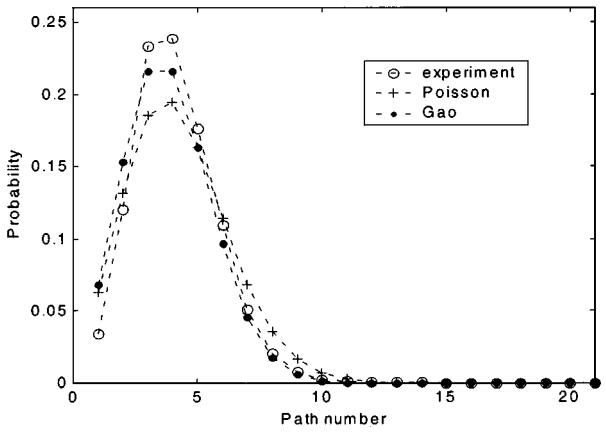

(a)

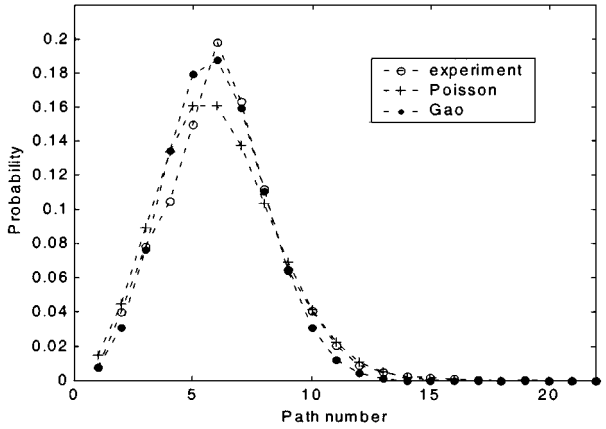

(b)

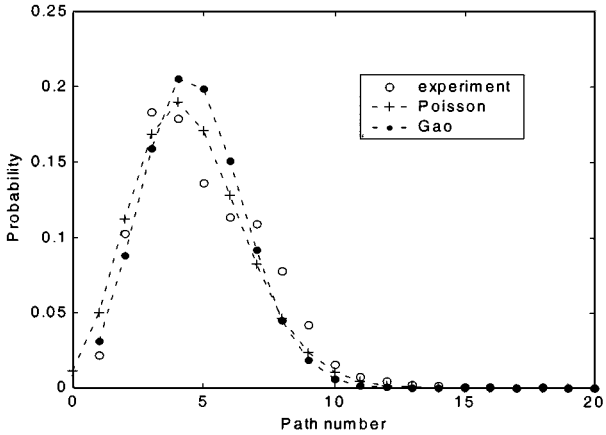

(c)

Fig. 10. Path number distributions. (a) Urban NLOS case with Tx height of 4 m. (b) Urban LOS case with Tx height of 45 m. (c) Suburban NLOS case with Tx height of 12 m.

and Table V show that both Poisson's and Gao's PDFs have good agreement with experimental values. However, Gao's PDF has been noticed to give better fit than Poisson's distribution especially at high probability values. The maximum path number that the mobile can receive is around 20, but the probability is very small for the path number greater than 15. It can be easily proven by using the measured data that if the dynamic range is cut at different levels, for example, -25, -20 and -15 dB, the fitting parameters in (3) and (4)

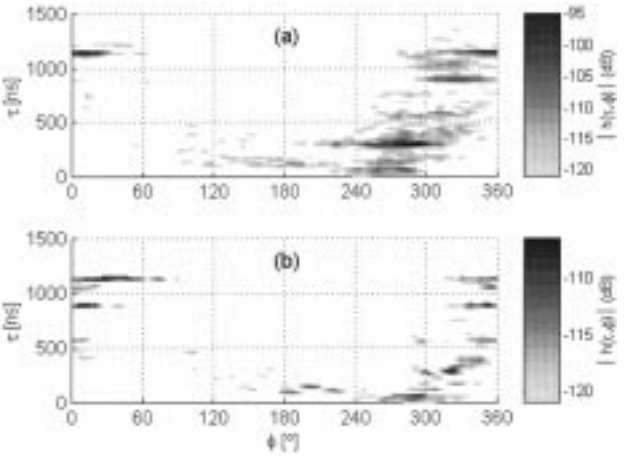

Fig. 11. Relative amplitudes for measured IRs using different elevation angles of the horn antenna. (a) 0°. (b) 30°.

will be changed, but the path number distributions still follow Poisson's and Gao's distributions.

VIII. Rotation Measurements in an Urban Environment

The rotation measurements at points P_1 and P_2 were performed at Site C shown in Fig. 2. The transmitter height was 12 m and the receiver was on a rotating stand at the height of 1.6 m and close to the receiver is a large open square. In the experiments, large excess delays up to 1.2 μs and rms delay spread about 0.42 μs are found, which are shown in Figs. 11(a) and (b) and 12, respectively. The power angular profiles (PAPs) $P_r(\phi)$ of the measurements were calculated by using the maximal ratio combining algorithm in the delay domain [16]

$$P_r(\phi) = \alpha_{\text{cal}} \int_{\tau_{\min}}^{\tau_{\max}} |h(\tau, \phi)|^2 d\tau \tag{6}$$

where α_{cal} is a factor which is obtained from the calibration measurement with a cable and an attenuator, and $\tau_{\min}$ and $\tau_{\max}$ are the delays of the first and last detectable IR components, and ϕ is the angle of arrival of the waves in the azimuth plane. In the rotation measurements, the dynamic range is cut at -26 dB relative to the strongest path. Fig. 12 shows two plots for rms delay spread corresponding to the elevation angles of 0° and 30°, respectively. The elevation angle of the horn antenna is defined as the angle between the horn axis and the azimuth plane.

Fig. 13 shows the PAPs for two elevation angles of the horn antenna. Strong signals can be found around 0°–30° and 260°–310° while the elevation angle of the horn is 0°. From Fig. 2, it is seen that around 0°–30° the signals are from the reflections of the far buildings, and around 260°–310° the strong signals are from diffractions and reflections of the nearby buildings. It is seen in Fig. 13, that the received power is decreased as the elevation angle of the horn antenna is increased. Fig. 14 shows the path number as a function of the rotation angles. It is seen that there are more multipath rays when $270° < \phi < 360°$, which is due to the diffractions and reflections from nearby buildings, and the multipath number is obviously reduced as the elevation angle is increased at 30°. This shows that when both transmitter and receiver are below

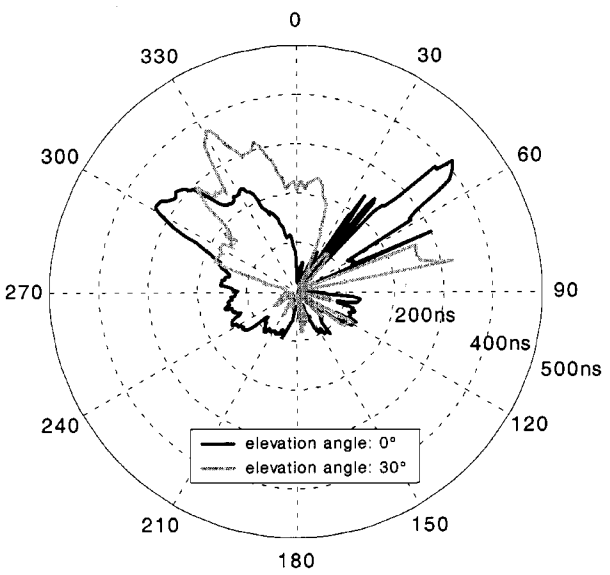

Fig. 12. Rms delay spread with different rotation angles in the azimuth plane.

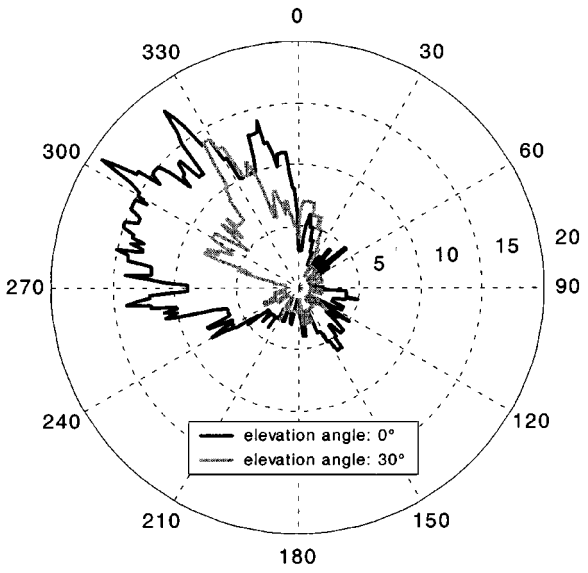

Fig. 14. Numbers of paths with different rotation angles in the azimuth plane.

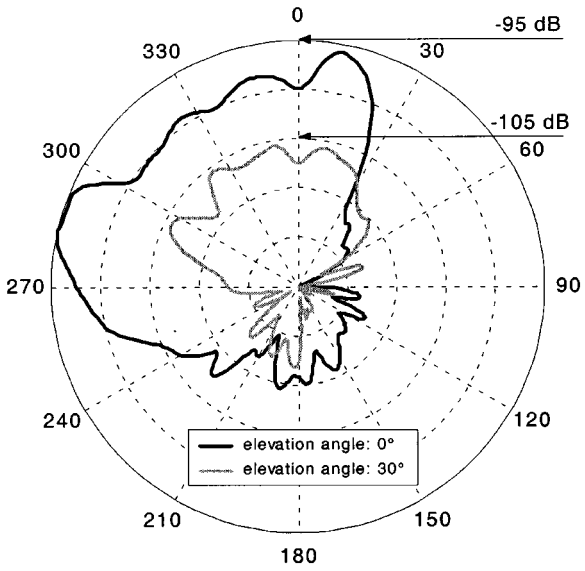

Fig. 13. Angular profiles of relative received power.

the rooftops, horizontal multipath propagation is dominant. Figs. 11–14 give the measurement results for point P_1, but there are no large differences between the measurement results in the two nearby points P_1 and P_2.

IX. Conclusion

The empirical channel models and parameters for wideband outdoor mobile communications at 5 GHz are given in this paper. The path loss exponents and intercepts are obtained by using the least square method. The exponents are within 1.4–3.5 in LOS and 2.8–5.9 in NLOS, respectively. The measurement distances are within 30–300 m in this experimental campaign. The mean excess delay and mean rms delay spread are within 29–102 ns and 22–88 ns, respectively. Large excess delays up to 1.2 μs and rms delay spread about 0.42 μs were found in the urban rotation measurements where the receiver is close to a large open square with surrounding buildings. A suitable window length is 1–2 m to average out fast fading components for micro- and pico-cells at 900 MHz–5 GHz frequency bands. The correlation distances at this frequency band with the correlation coefficient at 0.7 are between 1 to 11λ (about 0.06–0.62 m) and the correlation bandwidths at 0.7 are between 1.2 to 11.5 MHz. These correlation values strongly depend on the BS antenna heights. Both Poisson's and Gao's PDFs agree well with the experimental results. However, Gao's PDF is shown to be better than Poisson's distribution especially at high probability values. The PAPs and path number distributions with different elevation angles of the horn antenna show that when the heights of both the transmitter and receiver are below rooftops, the horizontal multipath propagation is dominant.

Acknowledgment

The authors would like to thank the reviewers for their helpful comments which improved this paper. They would also like to thank Prof. A. Räisänen for his encouragement and support. This work was performed mostly in ETX-LALAMO, a project on broadband wireless modems of the National Technology Agency of Finland (Tekes) coordinated by VTT Electronics and supported by Elektrobit Inc., Nokia Networks and Elisa Communications.

References

[1] *HIPERLAN*, Type 2 Functional Specification Part 1—Physical (PHY) Layer, 1999.
[2] "Wireless Access Method and Physical Layer Specifications," IEEE, New York, Rep. 802.11, Sept. 1994.
[3] F. J. Velez and L. M. Correia, "Classification and characterization of mobile broadband services," in *Proc. 52nd IEEE Vehicular Technology Conf.*, vol. 3, Boston, MA, 2000, pp. 1417–1423.
[4] L. M. Correia and R. Prasad, "An overview of wireless broadband communications," *IEEE Commun. Mag.*, vol. 35, pp. 28–33, Jan. 1997.
[5] G. Durgin, T. Rappaport, and H. Xu, "Measurements and models for radio path loss and penetration loss in and around homes and trees at 5.85 GHz," *IEEE Trans. Commun.*, vol. 46, pp. 1484–1496, Nov. 1998.

[6] N. Kita, K. Oosawa, A. Sato, H. Watanabe, and H. Hosoya, "Characterization of multipath delay profiles for a wideband wireless access system in a 5 GHz band," presented at the Proceedings of 10th IEEE International Symposium on Personal, Indoor and Mobile Radio Communications, Csaka, Japan, Sept. 12–15, 1999, paper number G5-2.
[7] K. Skog, A. Brehonnet, H. Kauppinen, and J. Kivinen. Wideband radio channel outdoor measurements at 5.3 GHz. presented at Millenium Conference on Antennas and Propagation Proceedings. [CD-ROM]paper number 1437
[8] W. C. Y. Lee, "Estimate of local average power of a mobile radio signal," *IEEE Trans. Veh. Technol.*, vol. 34, pp. 22–27, Feb. 1985.
[9] E. Green, "Radio link design for micro-cellular systems," *Br. Telecom. Technol. J.*, vol. 8, pp. 85–96, Jan. 1990.
[10] J. Kivinen, T. Korhonen, P. Aikio, R. Gruber, P. Vainikainen, and S.-G. Häggman, "Wide-band radio channel measurement system at 2 GHz," *IEEE Trans. Instrum. Meas.*, vol. 48, pp. 39–44, Feb. 1999.
[11] L. Juan-Llacer, L. Ramos, and N. Cardona, "Application of some theoretical models for coverage prediction in macrocell urban environments," *IEEE Trans.Veh. Technol.*, vol. 48, pp. 1463–1468, Sept. 1999.
[12] J. F. Lafortune and M. Lecours, "Measurement and modeling of propagation losses in a building at 900 MHz," *IEEE Trans. Veh. Technol.*, vol. 39, pp. 101–108, May 1990.
[13] V. Erceg, L. J. Greenstein, S. Y. Tjandra, S. R. Parkoff, A. Gupta, B. Kulic, A. A. Julius, and R. Bianchi, "An empirically based path loss model for wireless channels in suburban environments," *IEEE J. Select. Areas Commun.*, vol. 17, pp. 1205–1211, July 1999.
[14] D. C. Cox, "Delay Doppler characteristics of multipath propagation at 910 MHz in a suburban mobile radio environment," *IEEE Trans. Antenna Propagat.*, vol. 20, pp. 625–635, Sept. 1972.
[15] U. Dersch and E. Zollinger, "Physical characteristics of urban micro-cellular propagation," *IEEE Trans. Antennas Propagat.*, vol. 42, pp. 1528–1539, Nov. 1994.
[16] J. Kivinen, X. Zhao, and P. Vainikainen, "Empirical characterization of wideband indoor radio channel at 5.3 GHz," *IEEE Trans. Antennas Propagat.*, vol. 49, pp. 1192–1203, Aug. 2001.
[17] Y. Karasawa and H. Iwai, "Formulation of spatial correlation statistics in Nakagami-Rice fading environments," *IEEE Trans. Antennas Propagat.*, vol. 48, pp. 12–18, Jan. 2000.
[18] H. Suzuki, "A statistical model for urban radio propagation," *IEEE Trans. Commun.*, vol. 25, pp. 673–680, July 1977.
[19] S. Gao, "Study of Multipath Propagation in Land Mobile Communications," M.Sc. thesis (in Chinese), China Research Institute of Radio wave Propagation, Xinxiang, P. R. of China, 1995.
[20] S. Gao, S. Zhong, and C. Jiang, "Path number distribution for multipth propagation in land mobile communications and its simulation" (in Chinese), *J. China Inst. Commun.*, vol. 19, pp. 66–72, Feb. 1998.
[21] X. Zhao, J. Kivinen, P. Vainikainen, and K. Skog. Propagation characteristics for wideband outdoor mobile communications at 5.3 GHz. presented at Proc. of 4th European Personal Mobile Communications Conference. [CD-ROM]Paper pap21.pdf
[22] S. Y. Seidel and T. S. Rappaport, "914 MHz path loss prediction models for indoor wireless communications in multifloor buildings," *IEEE Trans. on Antennas Propagat.*, vol. 40, no. 2, pp. 207–217, Feb. 1992.
[23] J. D. Parsons, *The Mobile Radio Propagation Channel*. London: Pentech, 1992.

Xiongwen Zhao was born in Shanxi, China, in 1964. He received the M.Sci. and Lic. Tech. degrees (honors) from China Research Institute of Radiowave Propagation (CRIRP), Xinxiang, China, and Helsinki University of Technology (HUT), Espoo, Finland, in 1992 and 2001, respectively. He is currently pursuing the Dr. Tech. degree at the Radio Laboratory in HUT.

From 1992 to 1998, he was with the Ninth (Lab. of Troposphere Communications) and the Third (Lab. of Communications System Engineering) Laboratories in CRIRP, where he was a Senior Engineer and the Director of the Third Laboratory. His main fields of interest are wideband mobile propagation modeling and experiments, propagation in terrestrial microwave links, electromagnetic wave diffraction, and communications system engineering.

Mr. Zhao has received many awards from the Ministry of Electronics Industry of China and CRIRP for achievements in science and technology research.

Jarmo Kivinen was born in Helsinki, Finland, in 1965. He received the Master of Science in Technology and Licentiate of Science in Technology, and the Doctor of Science in Technology from Helsinki University of Technology (HUT), in 1994, 1997, and 2001, respectively, all in electrical engineering.

Since 1994, he has worked as a Research Engineer and Project Leader at Radio Laboratory of HUT, and 1-1/2 years as an RF Design Engineer at Nokia Telecommunications, Helsinki, Finland. His main fields of interest are in wideband radio channel measurement and modeling techniques, radio wave propagation, and RF techniques in radio communications.

Pertti Vainikainen (M'91) was born in Helsinki, Finland, in 1957. He received the M.S. degree in Technology, Licentiate of Science in Technology and the M.S. degree in Technology from Helsinki University of Technology (HUT), Espoo, Finland, in 1982, 1989, and 1991, respectively.

He worked at the Radio Laboratory of HUT from 1981 to 1992 mainly as a Teaching Assistant and Researcher. From 1992 to 1993, he was Acting Professor of Radio Engineering, since 1993, he was Associate Professor of Radio Engineering, and since 1998, he was Professor in Radio Engineering, all at the Radio Laboratory of HUT. From 1993 to 1997, he was the Director of the Institute of Radio Communications (IRC) of HUT. His main fields of interest are antennas and propagation in radio communications and industrial measurement applications of radio waves. He is the author or co-author of three books and over 110 refereed international journal or conference publications and the holder of four patents.

Kari Skog received his M.Sci. degree in applied physics from the Helsinki University of Technology (HUT), Espoo, Finland, in 1997.

From 1997 to 1998, he was with the European Laboratory for Particle Physics (CERN), Geneva, Switzerland, developing detectors and related electronics for high-energy physics experiments. In 1999, he joined the Nokia Research Center (NRC), Helsinki, Finland, where he started focusing on radio channel measurements, propagation modeling, and propagation research from the radio system point of view. Currently, he is concentrating on radio interface related performance issues in different radio network systems.